International Journal of Science and Research (IJSR)
ISSN (Online): 2319-7064
Index Copernicus Value (2016): 79.57 | Impact Factor (2015): 6.391

Calculate the Physical Properties for Samples of Active Galaxies Using Optical Spectroscopy Technique

Hasanain .H Al-Dahlaki

Department of Astronomy and Space, College of Science, University of Baghdad, Baghdad, Iraq

Abstract: ***Active galaxies are very special type of sources, where still many of their properties not fully understood yet. Therefore, in this project some of unstudied active galaxies are chosen and there are calculated physical properties, furthermore, the cooperation between the results are achieved. In this work three different types of active galaxies (Seyferts-I, Seyferts-II, and Quasars) are used. Each type is included three samples. The calculated properties for each samples are (Supermassive black hole mass, Eddington Rate, and the Luminosity distance) and the relation between these physical properties are discussed. The data in this project has been taken from "Sloan Digital Sky Survey SDSS", as a optical spectroscopic type. From the obtained results, the Supermassive black hole masses (SMBH) are heavier in the quasars with respect to the Seyferts type (1 and 2) Objects in a factor of 1.6 in average, and that will lead to another conclusion that the Star Formation Rate (SFR) in galaxies type quasars are higher than for galaxies type Seyferts (1 and 2). Also the relation between Star Formation (SF) and Supermassive black hole masses (SMBH) are calculated. Finally I have noted that with higher (SMBH) we will have high star formation rate (SFR).***

Keywords: active galactic nuclei, Star Formation rate (SFR), SMBH

1. Introduction

Active galaxies is not fully understandable yet and it is one of the most extreme, on the other hand it is highly distributed in the universe as known in the nucleus of these sources, there is a huge engine is laying.

The black hole is an object that is very huge, and miniature even from radiation of electromagnetic, like visional light, cannot get away outside. SMBH is amalgamation of tiny dimension, very powerful field of gravitational due to produce the enticing such as component key of the incentive that has superpowers AGN [1].

Unprecedented notes indicate the presence of masses with super massive black hole (SMBHs) masses $\geq 10^9$ $M_\odot$ as untimely has z $\geq$ 7. Their presence itself set the powerful restraint on the path of fountainhead and structure trail of supermassive black holes, from the desired time for the formation like huge target to the black hole BHs kernel (~ 100 $M_\odot$)[2].

In another wise, the superlative of the luminosity of Eddington for 10^4 $M_\odot$ black hole the Proposal has been unveiled as proof of intermediate-mass black holes (IMBHs), e.g. the exporter ESO 243-49 HLX1 with LX~10^{42} erg s^{-1}, and a black hole mass of MBH~ 104{105$M_\odot$ in a cluster with a stellar mass of M* ~10^5 – 106 $M_\odot$ {106$M_\odot$} has examined by [3].

For all that, NGC 5643 ULX1 with $L_X \sim 10^{40}$ erg s^{-1} styled a 30 $M_\odot$ That take place super-Eddington increase or Steaming emission advantageous towards.

Based on a belief that supermassive black holes (BHs) accumulated go on that engine that command quasars and active galactic nuclei (AGNs). Supermassive black hole (SMBHs) $\geq 10^9 M_\odot$ is confirm to be located in quasars centers detected stations so far redshift z ~ 7 [4].

The discovery of the 10^9 $M_\odot$ SMBHs in such a case be great redshift *z* form a main conjectural problem, see [5].

The accumulation is a supermassive black hole as energy sources of AGNs. Supports energy production accumulated disks powerfully on the construct and radiation of efficiency, that is fundamentally supervised by the Eddington, explain via measurement formation rate $\dot{m}=\dot{M}/\dot{M_{Edd}}$ where $\dot{M_{Edd}} = 1.39 \times 10^{18} \eta_{-1}^{-1} \left(\frac{M_{BH}}{M_\odot}\right) g\, s^{-1}$, $\dot{M}$ is the accretion rate [6].

Formation rate possess understood in order to apparent countenance of AGNs and can be known by $\dot{m}$. For all that it is difficult to evaluation by the observation [7].

In another hand, it is for fundamental guide that supermassive black holes (SMBHs) together the masses in a domain 10^6 – 10^{10} $M_\odot$ occur, it is incentive so as to force active galactic nuclei (AGNs) and quasars. Added to a lot of information that SMBHs establish in the center position of considerable, possibly generality galaxies, counting the Milky Way [8].

From Another side, The subsistence of chap massive stars have been orbit on irregular installment during a little tenths of a parsec of the supermassive black hole (SMBHs) in the centre of active Galaxy is brave for notion of star formation.

The abounding elevation snip separating the black hole have to rupture aloof of the clouds of molecular that form stars, abroad in the Galaxy, whilst carry the stars to the middle of

the galaxy as well evidence afield through their stellar existence [9].

Star formation has been an augmentation disk concerning the supermassive black hole is contingent whether the disc is satisfactorily massive, and if the star is capable to stimulate suitably fast [10].

I begin this project by calculate the supermassive black hole for sample of active galaxies, then calculate the other physical properties that related to what I mention previously, e.g. (Star Formation Rate (SFR), Eddington Rate (η), Luminosity distance (D_L)). Furthermore, finding a correlation between these physical properties.

In this paper the obtained results are included in the tables of information for the galaxies that I achieved from the SDSS survey. And my selection is based on three types of active galaxies: Seyfert Galaxies (Type I, Type II), and Quasars, and each type of galaxy I includes three samples.

1.1 The Sloan Digital Sky Survey

The Sloan Digital Sky Survey (SDSS) is an initial data liberation supply a database of 106000 unrivaled galaxies in the central galaxy pattern through unrushed spectrum.

As known The Sloan Digital Sky Survey (SDSS) is a delicate optical imaging and spectroscopic communal analysis of about 104 square degrees of the northern [11].

SDSS contributes the data to facilitate the complicated inquiries of the apportionment of luminous and no luminous element in the cosmos. It equips images and the photometry criterion validity in five bands (u, g, r, i, and z) at an average seeing of 1.5″, the minimal to a limiting factor of the magnitude is ∼22.2 in *r* band. The R ∼ 2000 spectroscopy overlays a wavelength domain from 3800−9200 Å [12].

SDSS commenced its procedure in May 2000. I used the ninth data release of the SDSS. Magnitudes for J0808 in the five SDSS qualifications are given in Table 1. Figure 2 shows the i-band SDSS optical image of the galaxy.

1.2 Sample selection and data reduction

These sources has been selected depending on the criteria that these sources never has been studied in detail. Therefore, I decide to focus on these objects.

As it was mentioned before the spectroscopic data has been taken from SDSS survey. Such kind of information need to be correct from stellar continuum and the emission-lines has to be fitted using Gaussian function.

The measurements of the line flux – emission have been established on alterations are depends of two codes: the Penalized PiXel Fitting codes and the absorbers of Fitting Line code to estimate kinematics of stellar and to conclude the properties of resurrection line [13].

GANDALF suits inhabitants of stellar and Gaussian resurrection line model to the concurrently chain of the galaxy due to individual continuum stellar and imbibitions lines from the reacted gas release.

The production via such fitting practicability contains emission-fluxes line, an E (B-V) rate and derived BPT sorting. The rouging amount ability to be acquired by sealing the E (B-V) rate for every target inside the easement of dust equation [14].

Lines resurrections are much weakened to become discover in BOSS. Plausible AoN rate could gain in a substitute of BOSS galaxies, for all that, for several of the powerful lines like the barred lines [OIII] 5007 and [NII] 6583, added the Ballmer lines Hβ and Hα. Finally the data in this project has been selected from this catalogue [15].

1.3 Physical Properties Calculations

1.3.1 Supermassive Black Hole (SMBH)

There are many evidence refer that all active provenance host a supermassive black holes in centrality of these galaxy [16] and the such part of this galaxies recognize as an engine from this sources. Mostly, supermassive black hole with a view to locate at midst of the host have been knowing now as real actuality that construction from the spirally pattern puffiness galaxy with elliptic (Massive black hole in midst of source is now famed acting as natural, supposedly pervasive, component of elliptical galaxies and spiral galaxy bulges).

Here, I calculate massive black hole for samples via dealing through calibration the relationship among the black hole mass with a velocity of stellar scuttle of sources relative puffiness component.

To compute the super massive black hole mass of the active galaxies, this formula is applied [17]:

$$\log\left(\frac{M_{BH}}{M_{\odot}}\right) = 8.12 + \log\left(\frac{\sigma}{200 kms^{-1}}\right)^{4.24\pm0.41} \quad (1)$$

This equation has been used to estimate the black hole mass via the dispersion velocity of [OIII] and [SII] emission lines. As shown in tables (1, 2 and 3), the velocity of dispersion σ has determined using Gaussian fitting for the SDSS survey. By applying these values (σ) for [OIII] with [SII], I estimate the masses of the SMBHs as presented in table (6)

1.3.2 Eddington Rate (η)

Eddington ratio η is a menstruation efficiency of the formation, due to the outflow radiation of the AGN that generated by isotropic emission of the maximum spherical accretion [18].

$$\eta = \frac{L_{bol}}{L_{edd}} \quad (2)$$

Equation (2) is the proportion between the bolometric luminosity L_{bol} and the Eddington luminosity L_{edd}.

The luminosity of bolometric commonly predestined for the band single menstruation. Rely on the energy of spectrum particular allocation; yonder huge doubt in correction of the bolometric for the isolated sources. Here, I appreciation the luminosity of bolometric, ensuing the instruction from [19].

Via utilize the comfort – structure of the 5100 Å density of luminosity.

$$L_{bol} \approx 9.47 * L_{\lambda}(5100A^{o})\ erg\ s^{-1} \quad (3)$$

Furthermore, The Eddington luminosity is calculated via the following relation [20]:

$$L_{edd} \approx 1.26 \times 10^{38} \times (MBH/M_{\odot}) erg\ s^{-1}. \quad (4)$$

The values of the (η) are listed in table (5).

1.3.3 Luminosity distance (D_L)

To determine the distance of luminosity for every source in this paper, I combine the values of red shift for each object with the cosmology constants H_0 = 70 km s^{-1} Mpc^{-1}, Ωm= 0.3 and ΩΛ = 0.7, which has been used throughout this work. I estimated the luminosity distance D_L via this formula [21]:

$$L_{(v)} = 4\pi \times D_L^{\ 2} \times S_{(v)} \quad (5)$$

Where *L* is Luminosity, *S* is the flux, where the results are included in table (4).

1.3.4 Star formation Rate (SFR)

Most of the active galaxies that have high radio emissions are distinguished by vigorous formation of the star activity. Nonetheless, this is to certify that issue of concentrated discussion as interactions between the jet and the source ISM, it also guides to extinction the star formation [22].

The galaxies that emits radiation with powerful lines in their spectra, where these lines come from the nuclei of the host have high activity of star-formation in factor of 3−4.

To calculate the star-formation rate for the optical data that has been involved in this work, I used [OII] λ 3728 emission line luminosity via this equation [23]:

$$SFR_{[OII]}[M_{\odot} yr^{-1}] = \frac{L_{[OII]}}{2.97 \times 10^{33} W} \quad (6)$$

2. Conclusions and Dissections

Through SDSS data, is achieved as show in this paper the calculation for the supermassive black hole mass (SMBH) Table 1. It is noticed from the calculation: The SMBHs of QSO sources are more massive than the other objects (Sy-I and Sy-I). Because the SMBH are related to the activity of active galaxies that means the QSQ galaxies are more active than (Sy-I and Sy-II) as shown the spectra intensity in Figure (1, 2, and 3). The SMBH masses of (Sy-I and Sy-II) are kind of equal, and that give us an indication that both type are actually the same type but it's matter of how is the galaxy is tilted to us (the observer). Eddington Rate is physical properties that relates to the SMBH. Therefore, I consider that the values of Eddington Rate is high in QSO sources more than the other types.

Additionally, in this paper, dealing with different type of galaxies (Seyfert-I, Seyfert-II, and QSO), when observed emissions lines ([O II], Hβ, [O III], Hα, [S II], [S II]), rest wave length Ao, dispersion velocity σ and flux density [10^{-17}erg. $^{cm-2}$. s^{-1}] in SDSS J000759.86+010423.6, SDSS J000813.22-005753.3, and SDSS J001056.25-090109.9 for Seyfert-I (see table 1).

I use The same parameter emissions lines ([O II], Hβ, [O III], Hα, [S II], [S II]), rest wave length Ao, dispersion velocity σ and flux density [10^{-17}erg. Cm^{-2}. s^{-1}] in SDSS J000026.31+003550.8, SDSS J000130.24-001446.4, and SDSS J000735.54+004744.8 for Seyfert-II ((see table 2), finally the parameter emissions lines ([O II], Hβ, [O III], Hα, [S II], [S II]), rest wave length Ao, dispersion velocity σ and flux density [10^{-17}erg. Cm^{-2}. s^{-1}] in SDSS J011110.04-101631.8, SDSS J105007.75+113228.6, and SDSS J080554.11+111432.4For QSQ (see table 3).

I extend within accurate authorization for defining the SFR for SDSS galaxies. The predictable muscular connection between [OII] and Hα fluxes line for SF galaxies is visible, however at a intermediate the flux line ratio, concerning an operator of two minimal in order that set up in the representative of Kennicutt (1992). This association applied in define the [OII] SFRs, is proportionate for the luminosity-following link set up by Jansen et al. (2000).

For the considerable model size and the comprehensive measured the spectroscopy accomplished via the survey, so it extend a large resource of realization of SF in the galaxy. All this agrees with (A. M. Hopkins et al, 2003).

The conclusion that Submitted by Xu et al. (2015)) Includes as well as studied by Hainline et al. (2013), the intensity of the [OIII] 5007 line is augment further fast than respectively to the luminosity of AGN (Xu et al. 2015)

At comparatively top of the redshift (with altitude luminosity of AGN), exposure emission of [OIII] of accessories of the host galaxy during the spectrography might participate to such effect.

Finally, as shown in this work that the Supermassive black hole masses (SMBH) are heavier in the quasars with respect to the other sources in a factor of 1.6. Additionally, that will lead to the higher Star Formation rate (SFR) in quasars than the other sources. That will lead us to another conclusion that there is a strong correlation between Supermassive black hole masses (SMBH) and Star Formation rate. Moreover, from all that above equations, the obtained conclusions and dissections lead to that higher (SMBH) will have higher start formation rate (SFR)(see table 4, 5 and 6).

References

[1] Laing, R.A., Jenkins, C.R., Wall, J.V., Unger, S.W., **2014**. The First Stromlo Symposium: The Physics of Active Galaxies. ASP Conference Series, **54**: p201.
[2] Kohei Inayoshi et al. **2014.**Formation of an embryonic supermassive star in the first galaxy, *Monthly Notices of the Royal Astronomical Society*. **445** (1):L109–L113.
[3] S. Komossa and D. Xu. **2007**. Narrow-line Seyfert 1 Galaxies and the MBH − σ Relation. *The Astrophysical Journal*, **667**:L33-L36. Doi: 10.1086/522002
[4] Lunan Sun et al. **2017**.Magneto rotational Collapse of Supermassive Stars: Black Hole Formation,

Gravitational Waves and Jets. *Physical Review D*.**96**(4): 43-52.doi: 10.1103/PhysRevD.96.043006.

[5] Różańska et al. 2017. Multiphase environment of compact galactic nuclei: the role of the nuclear star cluster. Monthly Notices of the Royal Astronomical Society. 464 (2): 2090–2102.

[6] Toshihiro Kawaguchi et al. **2004**. Growth of massive black holes by super-Eddington accretion. *Astronomy and Astrophysics*.**420** (3): 23-31.

[7] Ryan C. Hickox. **2013**. Supermassive Black Holes and the Growth of Galaxies. *The Astronomer*. **47**:274 – 327.

[8] R.E.A. Canning et al. **2013**. A multi-wavelength view of cooling vs. AGN heating in the X-ray luminous cool-core of Abell 3581. *Monthly Notices of the Royal Astronomical Society*.**435** (2): 1108–1125.doi.org/10.1093/mnras/stt1345.

[9] S. Nayakshin et al. **2009**. Massive black hole binary mergers within sub parsec scale gas discs. *Monthly Notices of the Royal Astronomical Society*. **393** (4): 1423–1432. *doi.org/10.1111/j.1365-2966.2008.14147*.

[10] Mattias Gustavsson. **2008**. *A quantum gas with tunable interactions in an optical lattice*. Ph.D. diss., Faculty of Mathematics, Computer Science and Physics, University of Innsbruck, Austria.

[11] Takashi Hosokawa et al.**2013**. Formation of Primordial Supermassive Stars by Rapid Mass Accretion. *The Astrophysical Journal*. **778** (2): 178 - 191.Doi: 10.1088/0004-637X/778/2/178.

[12] Zolt´an Haiman et al. **2013**.Growing Black Holes: Accretion in a Cosmological Context. In: The Growth of the Earliest Supermassive Black Holes and Their Contribution to Reionization. *Physics and Astronomy*. Springer, Berlin, Heidelberg, 30-41.

[13] Cappellari, M., et al. **2016**. Elliptical Galaxy Masses Out to Five Effective Radii: The Realm of Dark Matter. *Worldwide astronomical and astrophysical research*.**588**: 484, 493. Doi: 10.1051/0004-6361/201527807.

[14] Ana L. Chies-Santos et al. **2016**. OMEGA - OSIRIS Mapping of Emission-line Galaxies in A901/2: I. Survey description, data analysis, and star formation and AGN activity in the highest density regions. *Monthly Notices of the Royal Astronomical Society*. **450** (4): 4458–4474. Doi:10.1093/mnras/stv779.

[15] Y. Matsuoka. **2012**. Co-evolution of Galaxies and Central Black Holes: Observational Evidence on the Trigger of AGN Feedback. The *Astrophysical Journal*. **750** (1): 54 – 66. Doi: 10.1088/0004-637X/750/1/54

[16] M. Mechtley et al. **2016**. Do The Most Massive Black holes at z = 2 Grow via Major Mergers? *The Astrophysical Journal*. **830** (2). Doi: 10.3847/0004-637X/830/2/156

[17] Philip F. Hopkins et al. **2006**. Determining the Properties and Evolution of Red Galaxies from the Quasar Luminosity Function. T*he Astrophysical Journal Supplement*. **163**(1):50-79. Doi: 10.1086/499493.

[18] Suzy Collin et al. **2002**. Are quasars accreting at super-Eddington rates? Worldwide astronomical and astrophysical research.**388** (3):771 – 786. doi:10.1051/0004-6361:20020550.

[19] Genzel, Reinhard et al. **2010**. The Galactic Center massive black hole and nuclear star cluster. *Reviews of Modern Physics.***82** (4): 3121-3195. Doi: 10.1103/RevModPhys.82.3121

[20] Fernando Becerra. The black hole mass vs bulge velocity dispersion relation.

[21] P. Guillard et al. **2014**. Exceptional AGN-driven turbulence inhibits star formation in the 3C 326N radio galaxy. *Astronomy &Astrophysics*, **574**: A32 – A47. DOI: 10.1051/0004-6361/201423612.

[22] Narron, R., Ogle, P., &Laher, R. R. **2017**. Optimal Point-Source Extraction for Spitzer IRS Spectra. In ASP Conf. Ser. 376, ADASS XVI. San Francisco: 437- 440.

[23] P. Chris Fragile et al. **2016**. Numerical Simulations of a Jet-Cloud Collision and Starburst: Application to Minkowski's Object. *The Astrophysical Journal Supplement*. **201** (2): 9 – 20. Doi: 10.1088/0067-0049/201/2/9

Table 1: Shows the observed emissions lines for Seyfert-I: rest wave length, dispersion velocity and flux density.

SDSS J000759.86+010423.6				SDSS J000813.22-005753.3				SDSS J001056.25-090109.9			
Line name	Rest wave length A^o	σ	Flux [10^{-17}erg. Cm^{-2}. s^{-1}]	Line name	Rest wave length A^o	σ	Flux [10^{-17}erg. Cm^{-2}. s^{-1}]	Line name	Rest wave length A^o	σ	Flux [10^{-17}erg. Cm^{-2}. s^{-1}]
[O II]	3727	159.1	42.92	[O II]	3727	230.2	99.42	[O II]	3727	140.7	63.03
Hβ	4863	159.1	11.83	Hβ	4863	1448	463.1	Hβ	4863	1333	175.3
[O III]	5008	159.1	228.3	[O III]	5007	230.2	673.9	[O III]	5007	140.7	243.9
Hα	6564	141	290.9	Hα	6564	1448	3391	Hα	6564	1333	2293
[S II]	6718	159.1	54.26	[S II]	6714	230.2	164	[S II]	6714	140.7	82.75
[S II]	6732	159.1	42.81	[S II]	6732	230.2	132.2	[S II]	6732	140.7	66.48

Table 2: Shows the observed emissions lines for seyfert-II: rest wave length, dispersion velocity and flux density.

SDSS J000026.31+003550.8				SDSS J000130.24-001446.4				SDSS J000735.54+004744.8			
Line name	Rest wave length A^o	σ	Flux [10^{-17}erg. Cm^{-2}. s^{-1}]	Line name	Rest wave length A^o	σ	Flux [10^{-17}erg. Cm-^{2}. s^{-1}]	Line name	Rest wave length A^o	σ	Flux [10^{-17}erg. Cm^{-2}. s^{-1}]
[O II]	3727	197.6	131.9	[O II]	3727	132.7	77.26	[O II]	3727	140.1	37.01
Hβ	4863	205.5	46.78	Hβ	4863	126.7	69.86	Hβ	4863	166.9	31.07
[O III]	5007	197.6	603.3	[O III]	5007	132.7	379.4	[O III]	5007	140.1	213
Hα	6564	205.5	332	Hα	6564	126.7	265.7	Hα	6564	166.9	114.7
[S II]	6714	197.6	159.5	[S II]	6714	132.7	63.61	[S II]	6714	140.1	39.01
[S II]	6732	197.6	147.1	[S II]	6732	132.7	59.57	[S II]	6732	140.1	29.35

Table 3: Illustrate the emissions lines for QSO: rest wave length, dispersion velocity and flux density.

SDSS J011110.04-101631.8				SDSS J105007.75+113228.6				SDSS J080554.11+111432.4			
Line name	Rest wave length Ao	σ	Flux [10^{-17}erg. Cm^{-2}. s^{-1}]	Line name	Rest wave length Ao	σ	Flux [10^{-17}erg. Cm^{-2}. s^{-1}]	Line name	Rest wave length Ao	σ	Flux [10^{-17}erg. Cm^{-2}. s^{-1}]
[O II]	3727	6018	494	[O II]	3727	2029	2165	[O II]	3727	2071	533
Hβ	4863	1246	1645	Hβ	4863	800.8	7158	Hβ	4863	905.2	2907
[O III]	5007	6018	59.89	[O III]	5007	2029	2444	[O III]	5007	2071	506.1
Hα	6564	1246	9227	Hα	6564	800.8	1732	Hα	6564	905.2	7642
[S II]	6714	6018	3.935e+04	[S II]	6714	2029	4241	[S II]	6714	2071	1691
[S II]	6732	6018	3.522e+04	[S II]	6732	2029	2979	[S II]	6732	2071	1302

Table 4: Shows the type of sources: redshift, observation date, declination, right ascension and declination

Name of source	Type	Redshift (z)	Obs.date M / D / Y	D_L Mpc	RA hh mm ss	DE O ' "
SDSS J011110.04-101631.8	QSO	0.178	27/09/2000	861.0	01:11:10.04	-10:16:31.82
SDSS J105007.75+113228.6	QSO	0.134	31/03/2003	630.7	10:50:07.75	+11:32:28.66
SDSS J080554.11+111432.4	QSO	0.227	10/03/2005	1129.7	08:05:54.11	+11:14:32.49
SDSS J000759.86+010423.6	Sy-I	0.129	18/11/2001	605.2	00:07:59.86	+01:04:23.60
SDSS J000813.22-005753.3	Sy-I	0.139	18/11/2001	656.3	00:08:13.22	-00:57:53.36
SDSS J001056.25-090109.9	Sy-I	0.082	17/09/2006	372.9	00:10:56.25	-09:01:09.94
SDSS J000026.31+003550.8	Sy-II	0.104	28/09/2003	480	00:00:26.31	+00:35:50.82
SDSS J000130.24-001446.4	Sy-II	0.089	20/11/2003	406.6	00:01:30.24	-00:14:46.44
SDSS J000735.54+004744.8	Sy-II	0.101	18/11/2001	465.2	00:07:35.54	+00:47:44.89

Table 5: Calculation for sources: L_{edd}, L_{bol} the Eddington Ratio (η).

Type	Name	L_{edd}	L_{bol}	Eddington Ratio (η)
QSO	SDSS J011110.04-101631.8	$3.24 * 10^{52}$	$4.2 * 10^{44}$	$1.3 * 10^{-8}$
	SDSS J105007.75+113228.6	$3.02 * 10^{50}$	$1.63 * 10^{45}$	$5.4 * 10^{-6}$
	SDSS J080554.11+111432.4	$3.31 * 10^{50}$	$1.66 * 10^{46}$	$5.01 * 10^{-5}$
Sy-I	SDSS J000759.86+010423.6	$6.32 * 10^{45}$	$4.87 * 10^{44}$	0.077
	SDSS J000813.22-005753.3	$3.023 * 10^{46}$	$9.95 * 10^{44}$	0.033
	SDSS J001056.25-090109.9	$3.72 * 10^{45}$	$3.29 * 10^{44}$	0.088
Sy-II	SDSS J000026.31+003550.8	$1.62 * 10^{46}$	$2.93 * 10^{44}$	0.018
	SDSS J000130.24-001446.4	$2.95 * 10^{45}$	$2.101 * 10^{44}$	0.071
	SDSS J000735.54+004744.8	$3.72 * 10^{45}$	$1.63 * 10^{44}$	0.044

Table 6: The final obtained results from the calculations.

Type	Name	Log (SMBH/ [$M_\odot$])	SFR
QSO	SDSS J011110.04-101631.8	14.41 ± 0.1	14.75
	SDSS J105007.75+113228.6	12.39 ± 0.1	34.6
	SDSS J080554.11+111432.4	12.42 ± 0.1	27.4
Sy-I	SDSS J000759.86+010423.6	7.7 ± 0.1	0.633
	SDSS J000813.22-005753.3	8.38 ± 0.1	1.72
	SDSS J001056.25-090109.9	7.47 ± 0.1	0.353
Sy-II	SDSS J000026.31+003550.8	8.098 ± 0.1	1.22
	SDSS J000130.24-001446.4	7.37 ± 0.1	0.52
	SDSS J000735.54+004744.8	7.47 ± 0.1	0.323

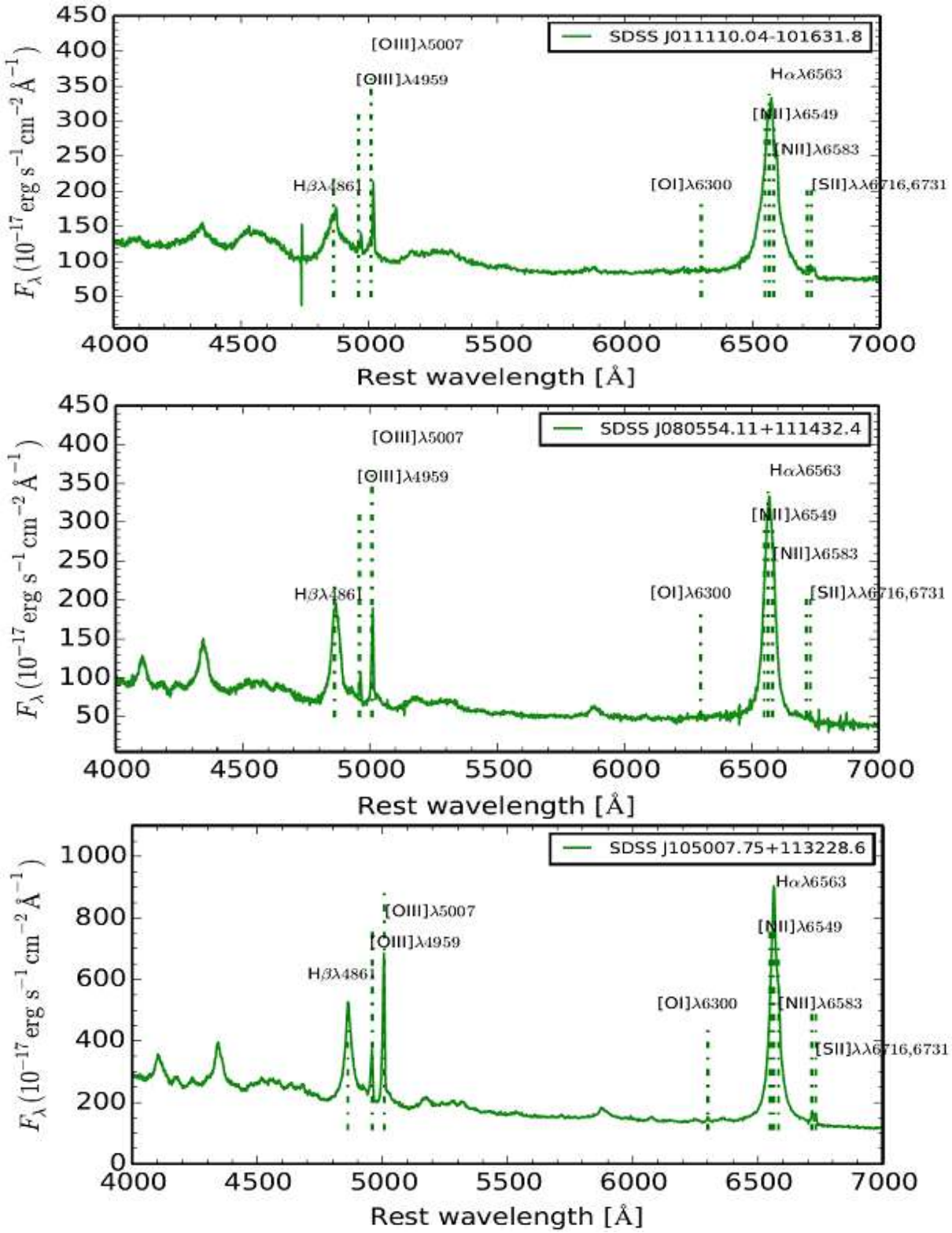

Figure 1: Shows the optical spectra of QSO.

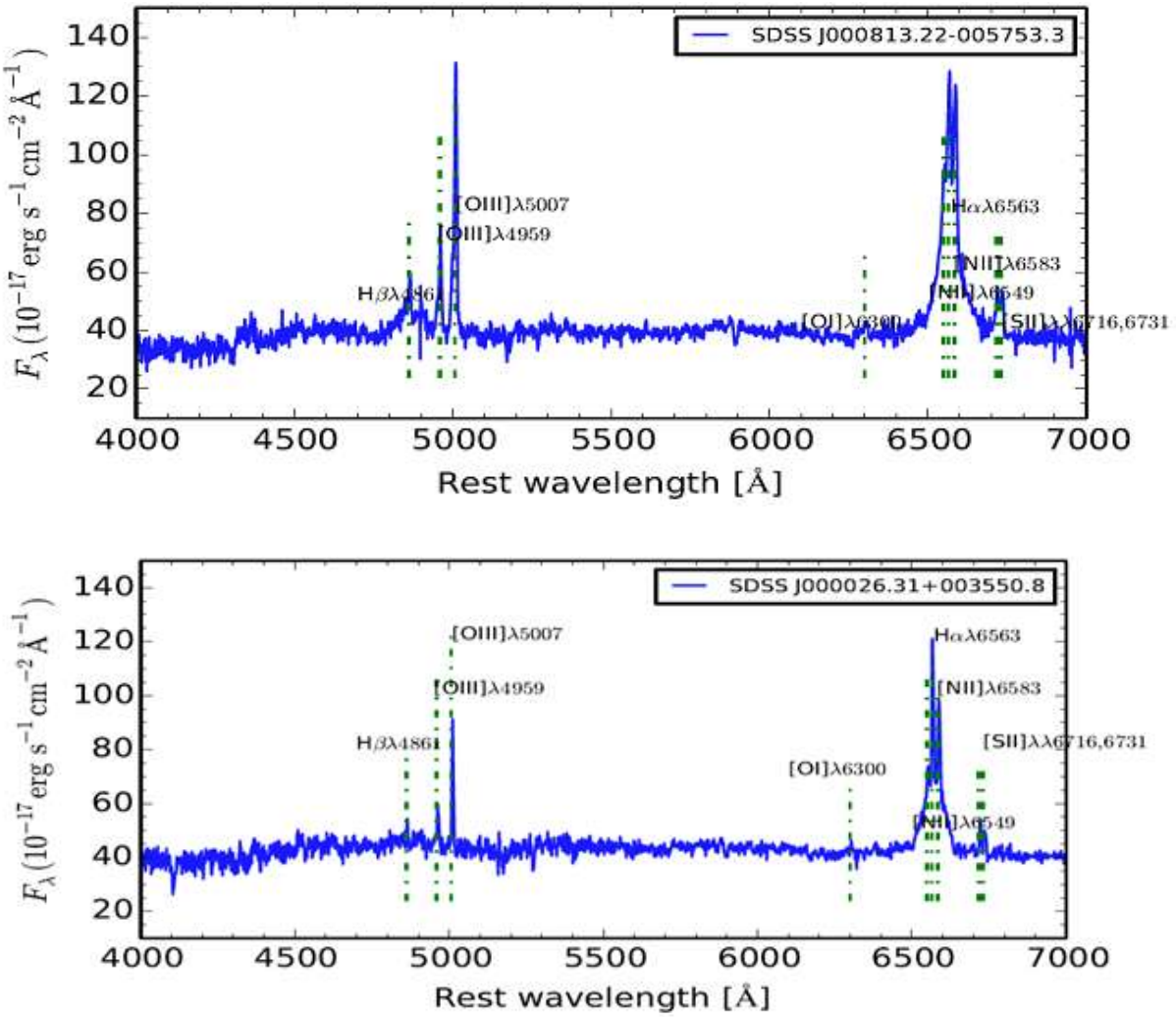

Figure 2: Shows the optical spectrum of Sey-I

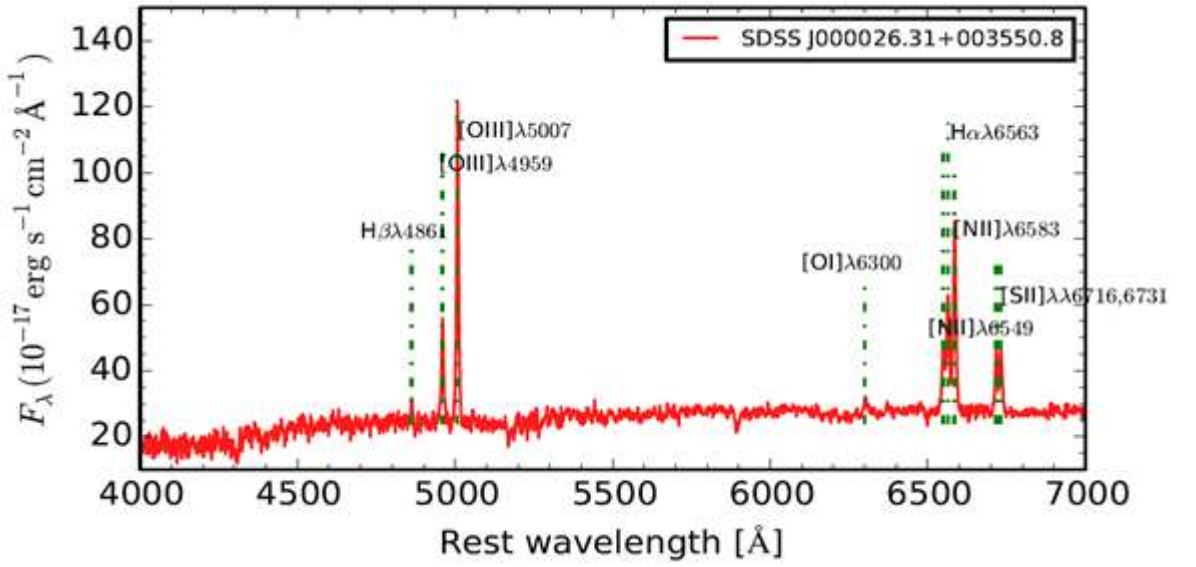

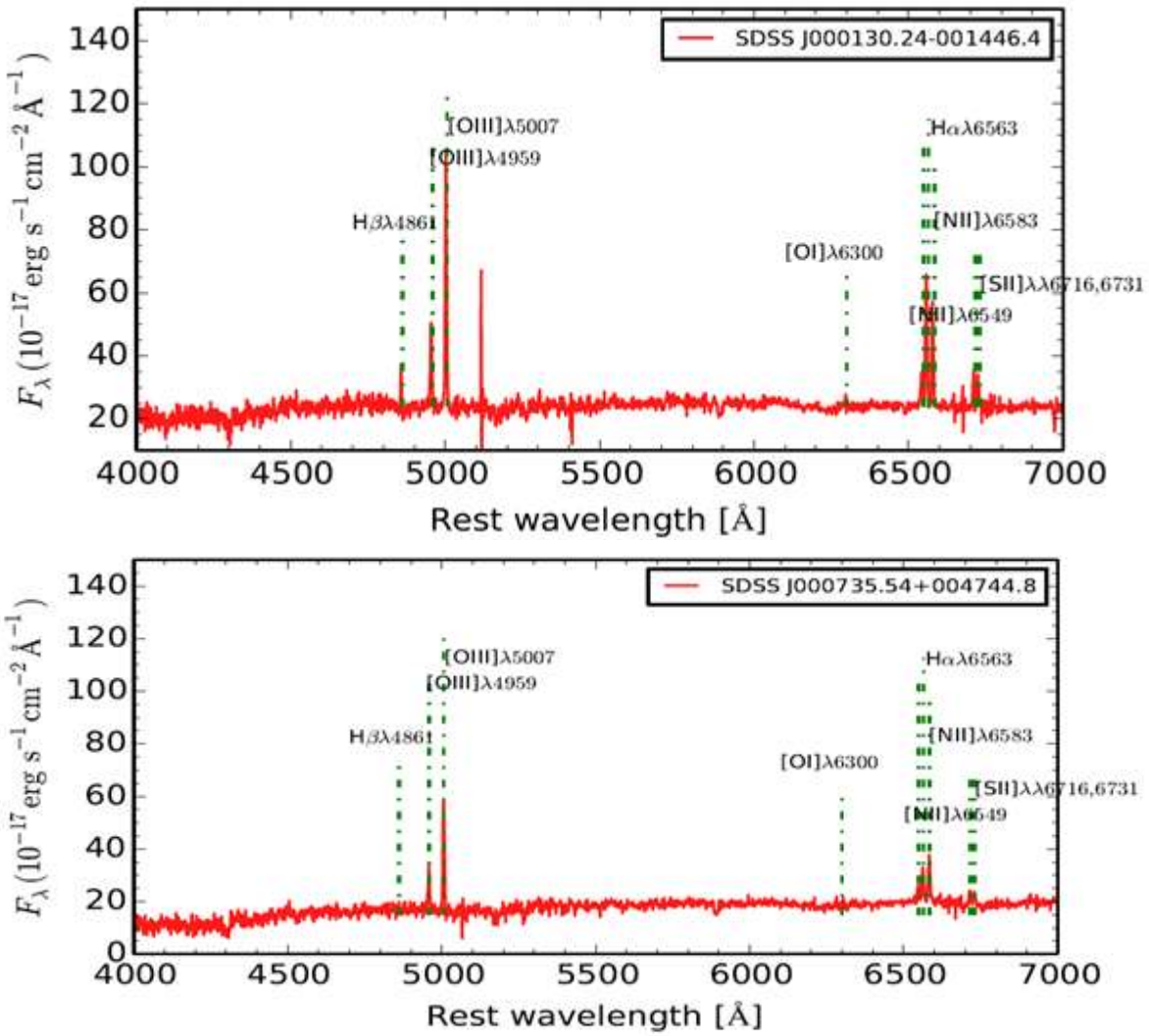

Figure 3: Shows the optical spectrum of Sey-II.